© 2018. Published by The Company of Biologists Ltd | Development (2018) 145, dev160325. doi:10.1242/dev.160325

RESEARCH ARTICLE

Lsd1 interacts with cMyb to demethylate repressive histone marks and maintain inner ear progenitor identity

Mohi Ahmed and Andrea Streit*

ABSTRACT

During development, multipotent progenitor cells must maintain their identity while retaining the competence to respond to new signalling cues that drive cell fate decisions. This depends on both DNA-bound transcription factors and surrounding histone modifications. Here, we identify the histone demethylase Lsd1 as a crucial component of the molecular machinery that preserves progenitor identity in the developing ear prior to lineage commitment. Although Lsd1 is mainly associated with repressive complexes, we show that, in ear precursors, it is required to maintain active transcription of otic genes. We reveal a novel interaction between Lsd1 and the transcription factor cMyb, which in turn recruits Lsd1 to the promoters of key ear transcription factors. Here, Lsd1 prevents the accumulation of repressive H3K9me2, while allowing H3K9 acetylation. Loss of Lsd1 function causes rapid silencing of active promoters and loss of ear progenitor genes, and shuts down the entire ear developmental programme. Our data suggest that Lsd1-cMyb acts as a co-activator complex that maintains a regulatory module at the top of the inner ear gene network.

KEY WORDS: Chick embryo, Epigenetic marks, Histone modification, Otic placode, Transcription factor

INTRODUCTION

In the developing embryo, multipotent progenitors are able to maintain their identity and gene expression programmes despite ongoing changes in their signalling environment. We have recently uncovered a gene network that integrates signalling inputs and transcriptional activity during the transition from progenitor to committed inner ear cells (Anwar et al., 2017; Chen et al., 2017), providing a good basis to explore this problem in a well-defined system. The entire inner ear is derived from a simple epithelium, the otic placode, located in the ectoderm next to the hindbrain. Prior to placode formation, otic precursors are part of a sensory progenitor pool (the pre-placodal region, PPR), from which FGF signalling induces otic-epibranchial progenitors (OEPs) (Anwar et al., 2017; Ladher et al., 2000; Maroon et al., 2002; Martin and Groves, 2006; Sun et al., 2007; Urness et al., 2010; Wright and Mansour, 2003). Over time, OEPs segregate into committed ear and epibranchial cells. They do this gradually by responding to new signalling cues and by altering their transcriptional machinery (Chen et al., 2017; Freter et al., 2008; Jayasena et al., 2008; Park and Saint-Jeannet, 2008; Sun et al., 2007). Thus, during this transitional period, OEPs must maintain their identity before proceeding to lineage commitment. The molecular mechanisms that maintain the competence of OEPs to respond to signals and maintain their progenitor state have not been identified.

Epigenetic mechanisms such as histone modifications are known to maintain progenitor cell identity as well as prime them for differentiation (Martin and Zhang, 2005), and may therefore play a role in keeping cells in an OEP state. One such modification is histone methylation in gene bodies and regulatory regions (Layman and Zuo, 2014; Ooi and Wood, 2007) that are associated with either gene activation or repression. In placode-derived sense organs, virtually nothing is known about the epigenetic control of cell identity as cells transit from progenitor to lineage commitment. The histone demethylase Kdm4b (also known as JmjD2B), which specifically removes di- and trimethyl groups from lysine 9 of histone 3 (H3K9me2/3) (Labbé et al., 2014), is the only epigenetic enzyme identified in inner ear precursors to date and controls placode invagination at later stages (Uribe et al., 2015). Recent RNA-seq analysis (Chen et al., 2017) identified the demethylase Lsd1 as specifically enriched in OEPs, suggesting that it could be involved in ear specification.

Lsd1 plays a key role in maintaining the pluripotency of stem cells (Adamo et al., 2011), as well as acting as a molecular toggle switch that promotes or inhibits differentiation of progenitor cells (Laurent et al., 2015). Lsd1 (also known as Kdm1a/Aof2/BHC110) is a flavin-dependent demethylase that specifically removes active H3K4me1/2 or repressive H3K9me1/2 marks, and thus can function as a transcriptional repressor or activator (Forneris et al., 2006; Metzger et al., 2016, 2005). Consistent with this, it is found in both co-repressor and co-activator complexes such as REST-CoREST (Ballas et al., 2005; Lee et al., 2005; Shi et al., 2005) and androgen receptor (AR)-Chd1 complexes (Metzger et al., 2016, 2005). Here, we show that Lsd1 is indispensable for ear development. It is required to maintain the expression of key progenitor-specific genes (*Sox8*, *Pax2*, *Etv4* and *Zbtb16*) that feed into a larger gene regulatory network that controls ear commitment. We identify cMyb as a novel Lsd1-interacting partner that recruits Lsd1 to promoter regions of actively transcribed genes to maintain the active histone mark H3K9ac by catalysing H3K9 demethylation.

RESULTS

Lsd1 is expressed in OEPs after their specification

The commitment of OEPs towards an otic fate is a gradual process that requires the integration and fine-tuning of gene regulatory networks (Chen et al., 2017). OEP specification by FGF signals begins around somite stage (ss) 1 in chick embryos (Groves and Bronner-Fraser, 2000). By ss5, OEPs express high levels of the FGF mediators *Etv4* and *Etv5* (Anwar et al., 2017; Betancur et al., 2011; Lunn et al., 2007), and develop along the otic lineage when cultured in isolation (Groves and Bronner-Fraser, 2000). However, it is not until ss10 that the otic lineage becomes molecularly distinct from

Centre for Craniofacial and Regenerative Biology, Floor 27 Tower Wing, Guy's Hospital, Dental Institute, King's College London, London SE1 9RT, UK.

*Author for correspondence (andrea.streit@kcl.ac.uk)

A.S., 0000-0001-7664-7917

Received 7 October 2017; Accepted 20 January 2018

Development (2018) 145, dev160325. doi:10.1242/dev.160325

the epibranchial cells (Chen et al., 2017), becoming fully committed to otic fate by ss11-12 (Groves and Bronner-Fraser, 2000). This progressive commitment is driven by a sequential activation of different signalling pathways (Freter et al., 2008; Jayasena et al., 2008; Park and Saint-Jeannet, 2008; Shida et al., 2015). The mechanisms whereby OEPs maintain their identity and remain poised for rapid response to new signals have not been identified.

We hypothesized that epigenetic mechanisms may be involved and, using our recent RNA-seq data (Chen et al., 2017), we identified *Lsd1* as a candidate for maintaining OEP identity prior to lineage commitment. *Lsd1* is expressed immediately after OEP specification but prior to molecular segregation of the otic-epibranchial lineages. We confirmed this by *in situ* hybridization. At ss5, *Lsd1* is confined to the neural tube, with weak expression in the mesoderm, but is absent from OEPs (Fig. 1A,a). At ss8, it becomes expressed in OEPs (Fig. 1B,b), and by ss13, it is robustly expressed in the otic placode and weakly in more lateral ectoderm (Fig. 1C,c). To determine the onset of *Lsd1* expression, we performed qPCR from dissected OEPs and placodes, and compared its expression with that of the transcription factor *Pax2*, an established, FGF-responsive OEP marker (Chen et al., 2017; Nechiporuk et al., 2007; Phillips et al., 2001; Yang et al., 2013). This analysis confirms the absence of *Lsd1* from OEPs at ss5 and its upregulation at ss8 (Fig. 1D), preceding the segregation of otic and epibranchial lineages. Thus, *Lsd1* expression is activated in OEPs after they have been specified, and its expression persists as otic cells become committed.

Lsd1 is necessary for otic placode formation and subsequent differentiation

To test directly whether *Lsd1* is required to maintain OEP identity, we performed knock-down experiments using two different morpholinos (MO) against *Lsd1* (Lsd1-MO; both affect *Lsd1* splicing; Fig. S1A). We find that Lsd1 knock-down with either MO leads to a dramatic reduction of otic vesicle size when compared with the control side (n=16, Fig. 2A-b′), indicating an important role for Lsd1 in ear development.

To understand global changes in the otic gene network after Lsd1 knockdown, we designed a NanoString probeset containing 220 transcripts based on our RNA-seq data (Chen et al., 2017), which includes 70 otic genes as well as factors specific for other placodes, neural, epidermal and neural crest cells (Table S1). Lsd1-MOs were electroporated into OEPs at ss5-6, and otic tissue was analysed after 4.5 and 9 h, corresponding to ss8-9 and ss11-12, respectively. Experiments were performed in triplicate and genes with a fold change of at least ±1.5 and $P \leq 0.05$ were considered to be deregulated (Table S2).

Several genes are rapidly upregulated after Lsd1 knockdown. These include the Notch targets *Hes4* and *Hey1* (a direct negatively-regulated Lsd1 target; Wang et al., 2007), the Notch ligand *Jag1*, and *Cbx4*, a component of the Lsd1-CtBP and the PRC2 co-repressor complexes (Shi et al., 2003; Tsai et al., 2010; Wang et al., 2007) (Fig. 3A).This is followed by increase of a number of lineage markers: the epidermal marker *Gata2* (Sheng and Stern, 1999), the neural crest genes *Snail1*, *Msx1* and *Id4* (Kee and Bronner-Fraser, 2001; Nieto, 2002; Streit, 2002), and the lens-specific transcripts *Pax6*, *Zeb2*, *L-Maf* and *C-Maf* (Bailey et al., 2006; Bhattacharyya et al., 2004; Lecoin et al., 2004; Sheng et al., 2003) (Fig. 3B). These data suggest that Lsd1 normally represses these transcripts and may prevent the switch of OEPs to other fates. By contrast, Lsd1 knockdown leads to loss of either OEP-specific genes (e.g. *Sox8*, *Pax2*, *Zbtb16*, *Etv4*) or genes that are already expressed at PPR stages (e.g. *Foxi3*, *Gbx2*, *Spry1/2*, *Six1*, *Eya2*, *Znf385c*), with *Sox8*, *Pax2* and *Spry2* showing the greatest fold change (Fig. 3A). Most of these genes are dependent on FGF signalling (Chen et al., 2017; Yang et al., 2013), and continue to be downregulated 9 h after Lsd1 knock down, when expression of additional downstream genes such as *Sox10* (a target of both *Sox8* and *Etv4*) (Betancur et al., 2011) are also reduced. These data indicate that Lsd1 is crucially required to maintain the transcriptional profile of OEPs, while simultaneously preventing alternative fates.

To validate the NanoString data and as an alternative approach to perturb Lsd1 function, we cultured OEP explants in the presence of tranylcypromine (TCP) – a well-documented Lsd1 inhibitor (Schmidt and McCafferty, 2007) – and then performed qPCR for selected genes. This approach verifies the downregulation of OEP and posterior PPR genes at ss8-9 (Fig. 3C, *Sox8*, *Pax2*, *Etv4*,

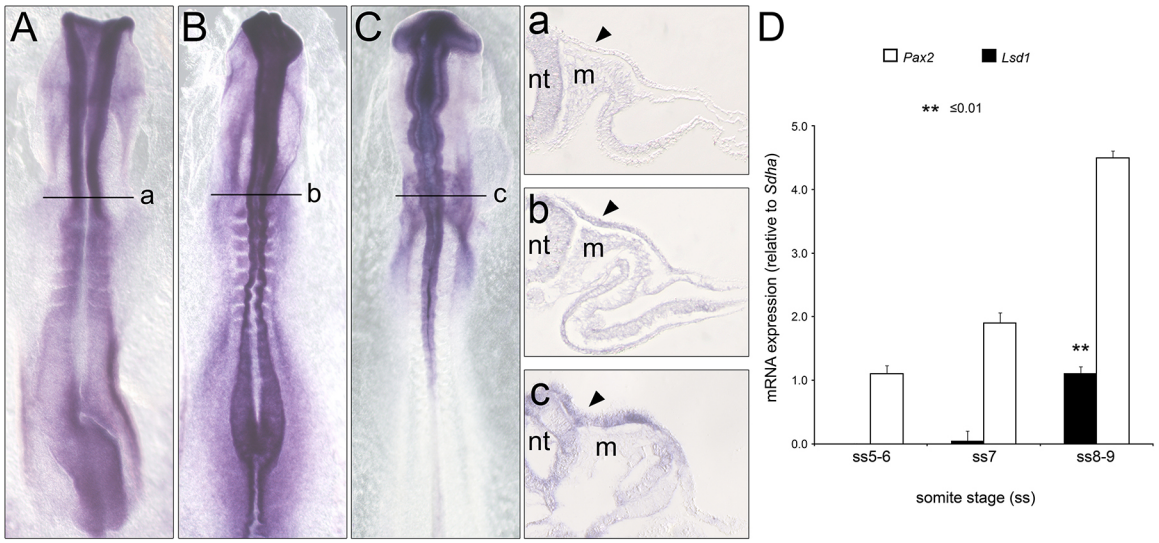

Fig. 1. *Lsd1* is expressed in progenitor cells after their specification. (A,a) At ss5, *Lsd1* is expressed in the neural tube (nt) and mesoderm (m) but not in otic-epibranchial progenitors (arrowhead). (B,b,C,c) At ss8 (B,b) and ss13 (C,c), *Lsd1* is expressed in the otic placode and lateral ectoderm (arrowheads). (D) The expression of *Lsd1* in OEPs begins at ss8-9 after OEP specification indicated by *Pax2* expression. *Sdha* was used as a housekeeping gene to determine the qPCR mRNA expression levels.

Development (2018) 145, dev160325. doi:10.1242/dev.160325

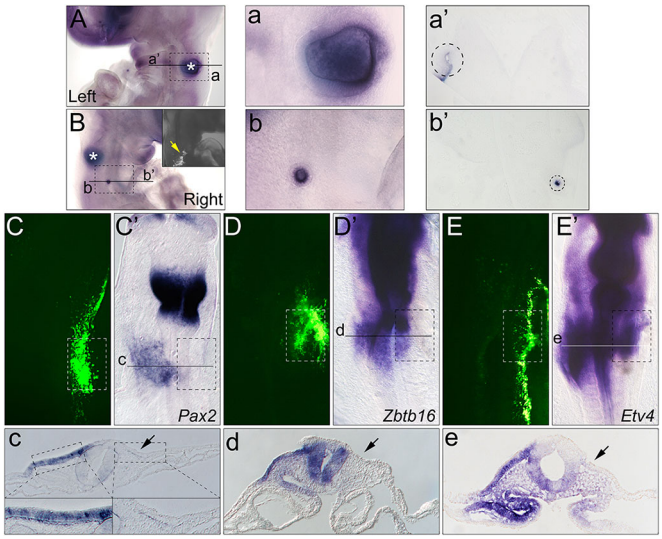

Fig. 2. Lsd1 is necessary for otic placode and vesicle formation. (A-b′) Left (A,a′) and right (B,b′) side of the same embryo. (A) Normal otic vesicle. (a) Higher magnification of the area boxed in A. (a′) Cross-section of region indicated by the line in A. (B) Lsd1-MO electroporated cells do not form an otic vesicle – only non-targeted cells (inset, yellow arrow) do. (b) Higher magnification of the area boxed in B. (b′) Cross-section of region indicated by a line in B. Asterisk indicates normal otic vesicle on the left side that can also be seen from the right side. (C′-E′,c-e) The expression of OEP markers is abolished on the side electroporated with Lsd1-MO (C-E; green). Black line indicates sectioned regions shown in c-e. Dashed boxes in C-E′ indicate the OEP region on the electroporated side; in c, insets show boxed regions at higher magnification.

Zbtb16, *Foxi3*, *Znf385c*) but not the upregulation of other genes (Fig. S1B). There is no increase in activated caspase 3 in Lsd1-MO targeted OEPs (Fig. S4), indicating that reduction of Lsd1 does not promote apoptosis but that, instead, OEPs lose their identity. Analysing OEP markers by *in situ* hybridization 9-12 h post MO electroporation reveals a complete loss of *Pax2* (n=8, Fig. 2Cc), *Zbtb16* (n=6, Fig. 2Dd) and *Etv4* (n=6, Fig. 2Ee) after Lsd1 knockdown, while upregulated genes cannot be verified (Fig. S1C,C′). Interestingly, although Lsd1-MO only target the ectodermal layer, *Etv4* expression is also affected in the underlying mesoderm and endoderm, pointing to reciprocal signalling between these layers and the placode. The epibranchial expression of *Pax2* is also abolished (Fig. 2C), and expression of other epibranchial markers such as *Foxi2* is reduced (n=5, Fig. S2D-d″). Morphologically, the placode is thinner, having lost the characteristic epithelial thickening compared with the control side (Fig. 2C-E; inset in Fig. 2C; Fig. S3I-L). Only cells that escape being targeted by Lsd1-MO maintain *Pax2* expression and coalesce to form a hypoplastic cup or vesicle (n=8, Fig. S2A-a; Fig. S3E-H), whereas control morpholinos (Ctrl-MO) do not affect normal placode involution into a cup (n=6, Fig. S2B,B′) or vesicle (n=4, Fig. S2C,C′). *Pax2* expression, loss of epithelial thickening as well as the late morphological phenotype can be rescued by co-electroporating Lsd1-MO with full-length human Lsd1-RFP (Fig. S3). Together, these data strongly support a role for Lsd1 in maintenance of the OEP transcriptional state and suggest that in this context it may act as a co-activator of OEP genes that determine OEP fate.

Lsd1 changes H3K9 modifications at OEP gene promoters

If Lsd1 functions as a direct co-activator of OEP and PPR genes, it should associate with their promoter regions to modify histone tails. To investigate this, we performed Lsd1 ChIP-qPCR on otic placodes and found that the promoters of *Sox8*, *Pax2*, *Etv4* and *Zbtb16* were bound by Lsd1, whereas promoters of *Spry2*, *Foxi3*, *Six1* and *Znf385c* did not show any significant Lsd1 recruitment (Fig. 4A, Fig. S5). Thus, OEP genes are direct Lsd1 targets, whereas PPR factors are likely to be regulated indirectly.

As a co-activator, Lsd1 acts by demethylating the repressive H3K9me2 found predominantly at silent promoters (Barski et al., 2007). H3K9 has a dual function at gene promoters, with opposing roles depending on its modification: acetylation is associated with gene activation, whereas methylation rapidly silences gene expression (Karmodiya et al., 2012). Thus, H3K9me2 demethylation by Lsd1 (Metzger et al., 2016, 2005) allows H3K9 acetylation, thereby maintaining an open chromatin state, while H3K9me2 accumulation in the absence of Lsd1 prevents H3K9ac and the chromatin remains closed (Fig. 4B). Indeed, when Lsd1 is

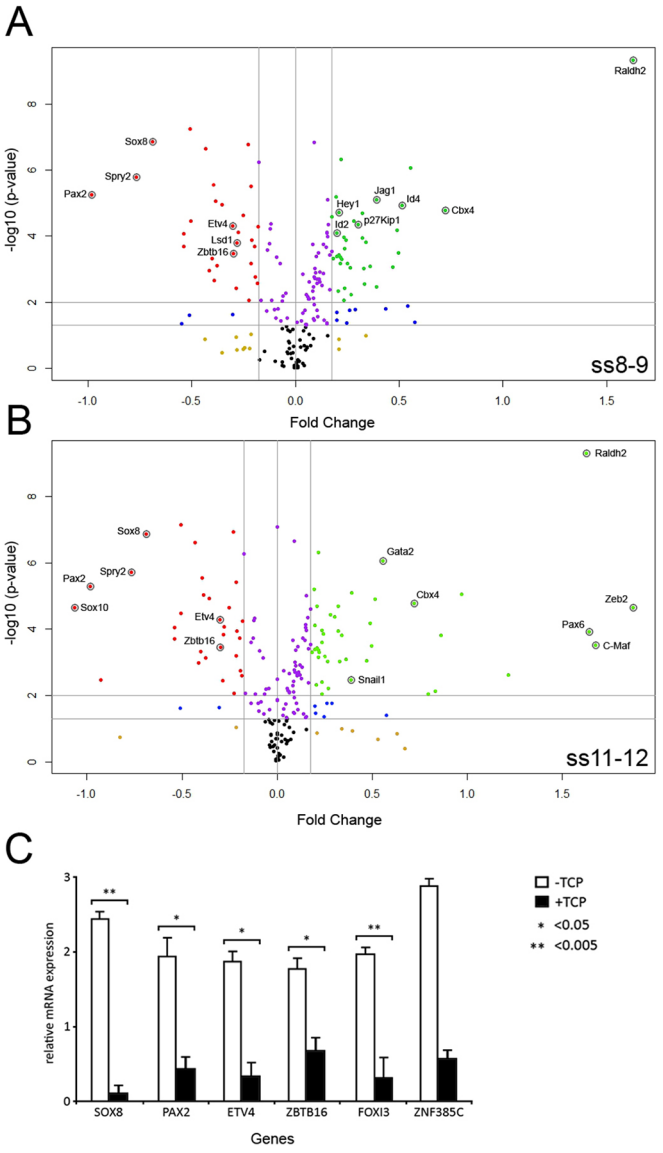

Fig. 3. Differentially regulated genes following Lsd1-MO knockdown. (A,B) Volcano plots representing changes in gene expression by NanoString analysis following Lsd1 knockdown at late OEP (ss8-9) and lineage-committed placodal (ss11-12) stages. Genes affected at ss8-9 are potential immediate targets of Lsd1. (C) Validation of selected genes by qPCR following pharmacological inhibition of Lsd1 with TCP. Experiments were conducted in triplicate and *Sdha* was used for normalization.

Development (2018) 145, dev160325. doi:10.1242/dev.160325

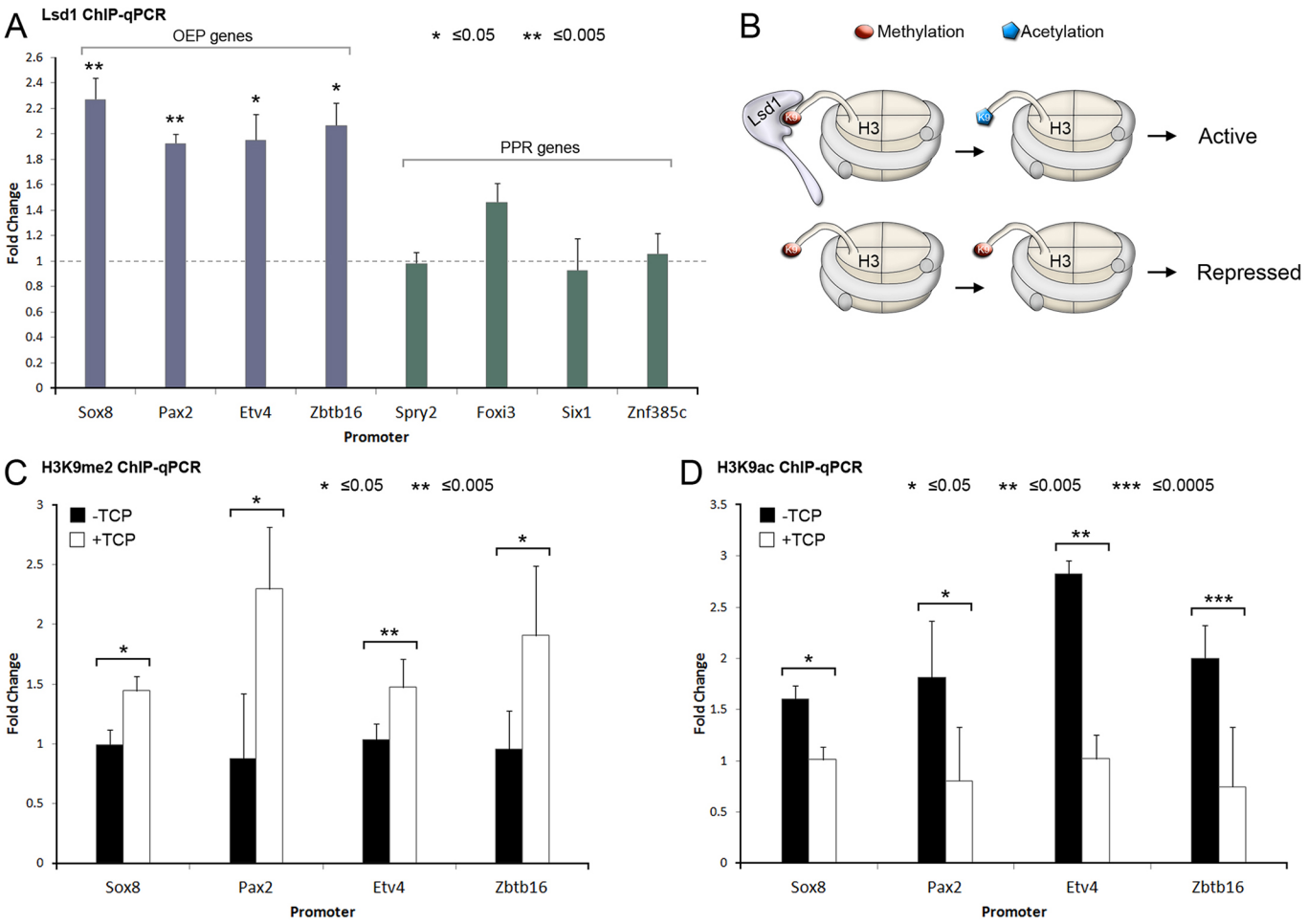

Fig. 4. Lsd1 occupies the promoters of target genes to remove H3K9me2. (A) Lsd1 ChIP-qPCR on promoters of genes that are downregulated after Lsd1 inhibition. Bar diagram shows relative enrichment of Lsd1 binding compared with IgG controls. Lsd1 binds to the promoters of OEP, but not to PPR genes. (B) To maintain active transcription, Lsd1 prevents accumulation of methyl groups on H3K9, thus allowing it to remain acetylated. In the absence of Lsd1, H3K9 methylation accumulates as H3K9ac is lost and the promoter is transcriptionally silenced. (C,D) ChIP for histone marks shows an increase of H3K9me2 at the target promoters following Lsd1 inhibition (C) and simultaneous loss of H3K9ac (D).

knocked down using MOs or inhibited by TCP, H3K9me2 increases in otic placode cells (Fig. S6). Importantly, using ChIP-qPCR for H3K9me2 and H3K9ac, we find that Lsd1 inhibition in OEP explant cultures by TCP results in an increase in H3K9me2 (Fig. 4C) and a corresponding decrease in H3K9ac (Fig. 4D) at the promoters of *Sox8*, *Pax2*, *Etv4* and *Zbtb16*. These data suggest that Lsd1 is normally recruited to the promoters of active OEP genes to prevent the accumulation of H3K9me2 and the loss of H3K9ac, thus allowing their continued expression.

cMyb interacts with Lsd1 and recruits it to target promoters

Lsd1 itself lacks the ability to bind DNA or to recognize the H3 tail within nucleosomes (Shi et al., 2005). How is Lsd1 recruited specifically to the promoters of OEP genes? As a co-repressor, Lsd1 interacts with the co-factor of REST (CoREST) via its chromatin-interacting SANT2 domain (Ballas et al., 2005; Lee et al., 2005; Shi et al., 2005) or with SNAG-domain transcription factors (such as Snail1/2 and Gfi1) (Lin et al., 2010; Saleque et al., 2007), which recruit Lsd1 to their respective target genes. To investigate which factor is responsible for recruiting Lsd1 to the promoters of *Sox8*, *Pax2*, *Etv4* and *Zbtb16*, we performed a motif enrichment analysis on these promoters using RSAT (Fig. 5A; Table S3). To narrow down potential Lsd1 partners in the ear, we removed factors belonging to the general transcriptional machinery and factors that are not expressed in OEPs. This strategy eliminates SNAG domain factors and hormone nuclear receptors, while returning Sox8, Pax2 as well as the SANT-domain containing coREST (via the presence of REST motif) and Myb as highly enriched motifs. Of those, Myb emerges as the top candidate to recruit Lsd1 to OEP gene promoters. Myb motifs are enriched in all four promoters (Fig. 5A), *cMyb* is expressed specifically in OEPs at ss5-6, just prior to *Lsd1* (Betancur et al., 2011); it contains a SANT domain and, together with its transactivation domain, can function as a co-activator or a co-repressor (Boyer et al., 2004). Morpholino-mediated knockdown of cMyb in OEPs at ss3-4 leads to the loss of Lsd1-targets such as *Pax2* (n=6, Fig. S7A-b) and *Zbtb16* (n=5, Fig. S7B,B′), but not of Lsd1 expression (Fig. S7C-J).

To assess whether cMyb and Lsd1 physically interact, we used lysates from neuroblastoma cells, which express these proteins in abundance (Fig. 5B), to perform co-immunoprecipitation. Although cMyb antibodies do not work in immunoprecipitation, Lsd1 antibodies successfully precipitate Lsd1 protein (Fig. 5B″). We therefore used Lsd1 antibody for immunoprecipitation followed by western blotting with cMyb antibody; this reveals that both proteins interact (Fig. 5B′). We then asked whether cMyb is required for Lsd1 binding to the *Sox8*, *Pax2*, *Etv4* and *Zbtb16* promoters.

Development (2018) 145, dev160325. doi:10.1242/dev.160325

A

TF	TF Motif	Promoters	p-Value	Expressed in OEPs?	Protein Complex with Lsd1?	Reference
MYB		*Sox8* *Pax2* *Etv4* *Zbtb16*	4.10E-05 1.80E-05 2.80E-05 3.20E-05	Yes - 5-6ss	Unknown	Betancur et al., 2011
PAX2	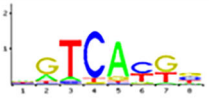	*Pax2* *Zbtb16*	4.60E-05 7.60E-06	Yes - 5-6ss	Unknown	Groves and Bronner-Fraser, 2000
SOX8	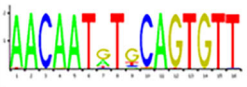	*Sox8* *Pax2* *Etv4*	5.40E-05 9.10E-06 7.50E-05	Yes - 5-6ss	Unknown	McKeown et al., 2005
REST	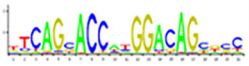	*Pax2* *Zbtb16*	1.10E-05 1.40E-05	ubiquitous	Yes, interaction with CoREST	Lee et al., 2005; Shi et al., 2005
AR	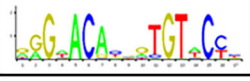	*Sox8* *Pax2* *Etv4* *Zbtb16*	2.00E-05 9.10E-05 3.70E-05 2.90E-05	No	Yes	Metzger et al., 2005

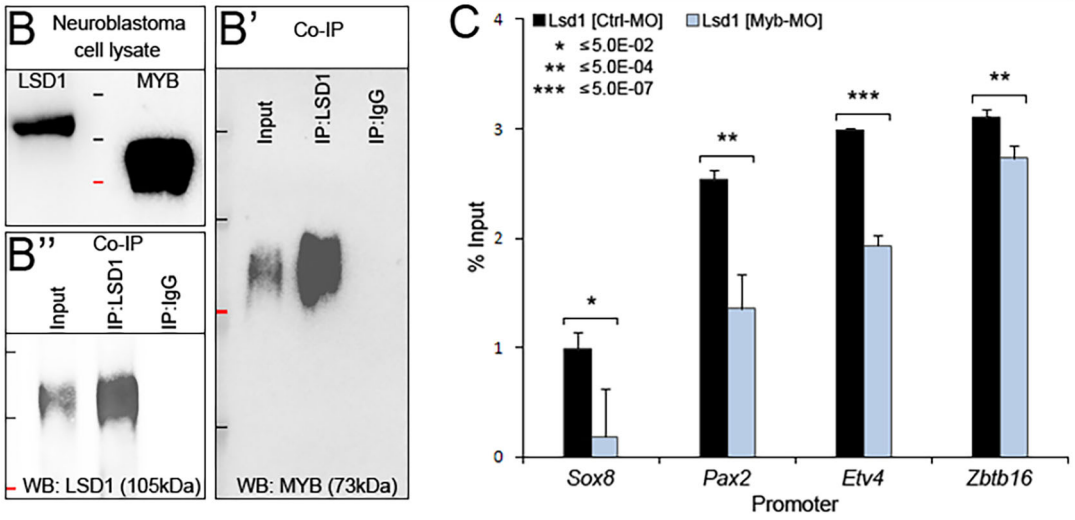

Fig. 5. Lsd1 interacts with cMyb, which recruits it to target promoters. (A) Motif enrichment analysis shows that a Myb-binding site is present in the promoters of all four OEP genes; cMyb is expressed at the appropriate time in the OEPs. (B) Neuroblastoma cell lines express Lsd1 and cMyb. (B′,B″) Immunoprecipitation with Lsd1 antibody followed by cMyb western blot reveals Lsd1-cMyb interaction. (C) Lsd1 promoter occupancy is lost following MO-mediated knockdown of cMyb.

Control or cMyb-MOs (Betancur et al., 2011) were electroporated into OEPs at ss3, targeted cells were harvested 10.5 h later at ss10 and processed for Lsd1 ChIP followed by qPCR for *Sox8*, *Pax2*, *Etv4* and *Zbtb16* promoter regions. Although Lsd1 binds all four promoters in controls, this is strongly reduced when cMyb is knocked down (Fig. 5C). Together, our data suggest that cMyb and Lsd1 proteins physically interact and that cMyb recruits Lsd1 to the promoters of the OEP genes *Sox8*, *Pax2*, *Etv4* and *Zbtb16*. In turn, this keeps H3K9 demethylated and allows its acetylation, thus maintaining OEP gene expression.

DISCUSSION

Although the epigenetic mechanisms that maintain stem cell pluripotency and the exit from this state *in vitro* are fairly well characterized, their role in controlling cell fate decisions and maintaining cell identity in normal embryonic development is much less understood. Here, we take advantage of the recently established gene regulatory network for ear development to investigate the epigenetic mechanisms that maintain ear precursors in a progenitor state prior to lineage commitment. Ear commitment is a gradual process that begins with OEP specification from a pool of sensory progenitors. Exposed to a changing extrinsic environment as morphogenesis proceeds, OEPs must stabilize their identity and retain competence to respond to signals that ultimately commit them to their fate (Fig. 6A). Here, we establish a central role for the demethylase Lsd1 in this process, driven by the transcription factor cMyb (Fig. 6B,C).

Lsd1 maintains the OEP module at the top of the inner ear regulatory network

The control of OEP specification and their subsequent commitment to either the otic or epibranchial lineages involves a hierarchical organization of gene regulatory networks and sub-networks. These network modules are interconnected and embedded within them are the signalling inputs that direct cell behaviour (Chen et al., 2017). Because of the hierarchical network organization and the crosstalk between regulatory modules, failure to maintain components of just one module will essentially shutdown the entire developmental programme. This is precisely what we observe in the absence of Lsd1 function. *Lsd1* expression is activated in OEPs after specification, and its expression persists in otic cells as they commit to their fate. Therefore, by directly maintaining the

Development (2018) 145, dev160325. doi:10.1242/dev.160325

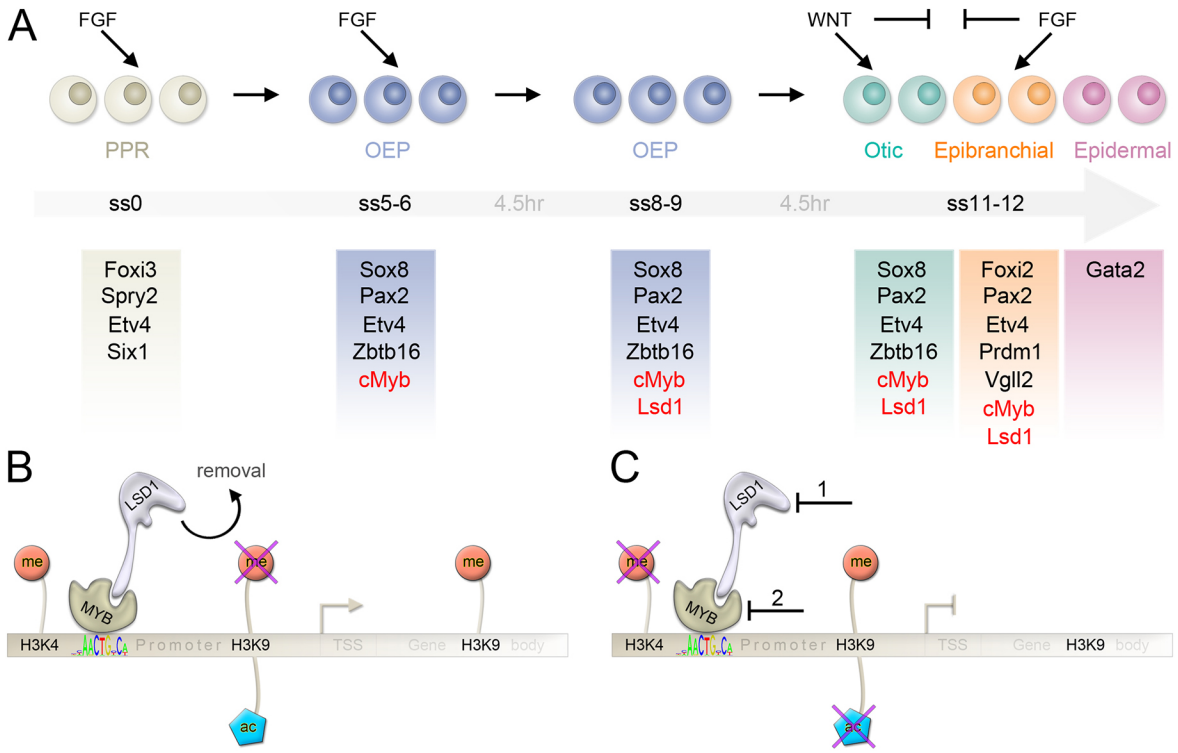

Fig. 6. Model for an Lsd1-cMyb co-activator complex in progenitor cell maintenance. (A) OEPs arise from sensory progenitors (PPR) identified by a set of genes. FGF activates OEP genes in the PPR; *cMyb* is not induced by FGF but becomes expressed at the same time. In a transitory state, OEPs upregulate *Lsd1* and maintain their identity until they respond to new signals and commit to a particular lineage by activating additional fate-specific genes. (B) cMyb recruits Lsd1 to active OEP promoters already decorated with H3K4 methylation and H3K9ac. To maintain their expression, Lsd1 prevents H3K9 methylation at the promoter, thereby allowing H3K9 to remain acetylated, and restricts H3K9me2 to the gene body. (C) Inhibition of Lsd1 (1) results in the loss of H3K9ac and gain of H3K9me2 at the active promoters, which are rapidly silenced and OEP gene expression is lost. Loss of cMyb (2) prevents the recruitment of Lsd1 to the promoters leading to the same outcome as Lsd1 inhibition.

expression of key players in the OEP module (*Sox8*, *Pax2*, *Etv4* and *Zbtb16*) that precede its own expression, Lsd1 becomes part of a sub-network that acts like a central hub for the entire ear cascade. Interestingly, these Lsd1 targets are dependent on FGF signalling for their initial expression, and Lsd1 is known to regulate both Wnt and FGF signalling pathways (Chen et al., 2016; He et al., 2016; Huang et al., 2017, 2013; Lei et al., 2015; Takeuchi et al., 2015).

In the zebrafish lateral line, Lsd1 is required to activate *Etv4*, *Axin2* and *Tcf7l2* to promote supporting cell proliferation upon hair cell damage (He et al., 2016), whereas it downregulates *Etv2* to promote commitment of hematopoietic progenitor cells to their fate (Takeuchi et al., 2015). Furthermore, in cancer cells, Lsd1 promotes the Wnt pathway by repressing negative regulators of Wnt/β-catenin signalling such as *APC*, *Prickle*, *Sfrp5* and *Dkk1* (Huang et al., 2017, 2013; Lei et al., 2015). In contrast, Lsd1 can also negatively regulate Wnt signalling by repressing Wnt pathway components such as *Fzd1/2* to promote mesenchymal stem cell differentiation into brown adipocytes (Chen et al., 2016). In the ear, Wnt signalling is required for the transition of OEPs to committed otic cells (Freter et al., 2008; Jayasena et al., 2008; Park and Saint-Jeannet, 2008). Thus, it is possible that maintenance of the OEP module by Lsd1 is necessary for OEPs to retain competence to respond to Wnt signalling and that Lsd1 directly or indirectly promotes the expression of Wnt pathway components.

Virtually nothing is known about the upstream regulators of *Lsd1*, although in our NanoString data, the expression of *Lsd1* itself is lost upon Lsd1-MO knockdown. As the expression of *Sox8*, *Pax2*, *Etv4* and *Zbtb16* in OEP cells precedes *Lsd1* expression, it is likely that one or more of these factors regulate *Lsd1* expression.

The Lsd1-cMyb co-activator complex prevents deactivation of OEP promoters

Lsd1 is a demethylase found in both activator and repressor complexes. Although the latter is well studied (Lin et al., 2010; Shi et al., 2005), its role as a co-activator is poorly defined. When Lsd1 is recruited by hormone nuclear receptors to their target promoters, its substrate specificity switches from H3K4me2 to H3K9me2 (Metzger et al., 2016, 2005). In turn, demethylated H3K9 provides a substrate for histone acetyltransferases, with H3K9ac at promoter regions being a hallmark for actively transcribed genes. In addition, the neuronal-specific isoform Lsd1+8a targets H3K9 for demethylation in the absence of nuclear receptors (Laurent et al., 2015). However, this isoform is found only in mammals and is absent in other vertebrates such as chick, fish and frog (Laurent et al., 2015; Zibetti et al., 2010). Our experiments reveal that Lsd1 can indeed switch substrate preference to act as a co-activator in the presence of cMyb.

In the otic placode, cMyb cooperates with Sox8 and Etv4 to control the expression of the late otic marker *Sox10*: cMyb knockdown results in *Sox10* downregulation and the loss of placode thickening (Betancur et al., 2011). This phenotype is remarkably similar to that produced by Lsd1 knockdown. Here, we show that Lsd1 and cMyb physically interact and that Lsd1 recruitment to its target promoters depends on the presence of cMyb. This finding suggests that both are part of the same molecular machinery that controls otic lineage commitment. As *Pax2* is expressed prior to *Lsd1*, we propose that Lsd1 can only function in OEP maintenance when both cMyb and Lsd1 are present. *Pax2* expression is initiated by FGF and one study suggests that this pathway must be downregulated (Freter et al., 2008) for cells to commit to the otic lineage. This coincides with the onset of

Development (2018) 145, dev160325. doi:10.1242/dev.160325

Lsd1 expression, and it is therefore possible that Lsd1 acts to maintain *Pax2* when FGF signalling begins to decline.

At promoter regions of OEP genes, Lsd1 prevents accumulation of the repressive mark H3K9me1/2 through its demethylase activity, allowing H3K9ac accumulation. cMyb is likely to play a key role to facilitate this. Unlike the chromatin-interacting SANT domain, which facilitates histone deacetylation by HDACs (Boyer et al., 2004), the cMyb SANT domain binds DNA and cMyb recruits the histone acetyltransferase p300 via its transactivation domain (Mo et al., 2005). In contrast, high levels of H3K9 methylation are essential along the gene body of actively transcribed genes and this is facilitated by histone methyltransferases such as Setdb1 or Ehmt2 (also known as G9a) (Layman and Zuo, 2014; Ooi and Wood, 2007). During adipogenesis, Lsd1 opposes the activity of Setdb1 at target promoters to prevent premature differentiation (Musri et al., 2010). However, the precise mechanism of how this occurs and whether Lsd1 modifies Setdb1 itself or whether there is negative feedback between the complexes remains elusive. We therefore suggest that the Lsd1-cMyb-p300 co-activator complex at the promoter region of OEP genes is crucial to counteract HDAC and HMT activities, and as a result prevents deactivation of OEP transcripts.

In addition, Lsd1 may also be part of a repressor complex, as HDACs and REST/coREST are present in OEPs, albeit being ubiquitously expressed in the embryo (Chen et al., 2017). In this context, Lsd1 may be important to repress non-otic genes, which may in turn prevent ear development. We have previously shown that, in the absence of additional signals, sensory progenitors in the PPR activate the lens programme through expression of the early marker *Pax6* and late lens genes such as *L-maf* and δ-crystallin. Lsd1 knockdown leads to the upregulation of lens genes, although at very low levels, and it is therefore tempting to speculate that Lsd1 is part of the machinery that prevents the lens default fate (Bailey et al., 2006). However, the upregulation of these genes is not maintained, possibly owing to inhibitory signals, and therefore the cells do not progress towards lens development. Together, our findings suggest that the Lsd1-cMyb-p300 co-activator complex lies at the heart of a mechanism that maintains OEP identity, and that Lsd1 is a molecular cell fate switch that ensures the execution of the ear programme.

Epigenetic regulation of cell maintenance and fate commitment in the embryo

Much of our understanding of the epigenetic regulation of cell fate decisions centres around maintenance of embryonic, neural or hematopoietic stem cells (Adamo et al., 2011; Foster et al., 2010; Sun et al., 2010; Takeuchi et al., 2015; Thambyrajah et al., 2016), cancer cells (Huang et al., 2017; Lei et al., 2015), and progenitor cell differentiation in the foetal or postnatal retina (Popova et al., 2016), anterior pituitary (Wang et al., 2007) or nervous system (Ballas et al., 2005). In all these cases, Lsd1 acts as a co-repressor to either maintain stem cell identity or to allow differentiation towards a particular fate, mostly targeting H3K4me1 at enhancer or H3K4me2 at promoter regions. However, there is limited evidence of the crosstalk between genetic and epigenetic regulation of cell fate in the developing embryo. To our knowledge, this is the first report that demonstrates a co-activator role for Lsd1 in cell fate maintenance. Our findings place Lsd1 within a gene regulatory network and show how a single epigenetic modifier maintains a network module that is in turn crucial to promote the ear programme. Many factors within this module are involved in other biological processes, cancer and/or mutated in human syndromes. Thus, from a therapeutic perspective, this study may provide insights into the mechanisms underlying the human syndromes caused by mutations in *LSD1* (Chong et al., 2016; Tunovic et al., 2014), such as cleft palate, psychomotor retardation and distinct facial features (CPRF; OMIM # 616728), as well as overlapping features with Kabuki syndrome (OMIM # 300867).

MATERIALS AND METHODS

Chromatin immunoprecipitation (ChIP)

Otic tissue collected in nuclear extraction buffer [10 mM Tris-HCl (pH 7.5), 3 mM $CaCl_2$, 250 mM sucrose, 0.5% NP-40, 0.25% Triton X-100, supplemented with 1 mM DTT and protease inhibitors (PIs)] was homogenized using a Dounce homogenizer on ice, crosslinked in 0.9% formaldehyde and quenched with 125 mM glycine. Nuclei were pelleted, washed in PBS (with DTT/PI) and lysed in SDS lysis buffer (50 mM Tris-HCl (pH 8), 1% SDS, 10 mM EDTA (pH 8), PIs] on ice for 1 h to release crosslinked chromatin. The chromatin was then sonicated using SorvicsVibra Cell and probe CV18 on ice in ChIP buffer without DTT [16.7 mM Tris-HCl (pH 8), 0.1% SDS, 1.2 mM EDTA (pH 8), 167 mM NaCl] to obtain DNA fragments of 0.2-1 kb. Fragmented chromatin was diluted in ChIP buffer with 1 mM DTT and PIs. Protein A magnetic beads (Invitrogen 10002D) were blocked in 0.5% BSA/PBS, incubated with 5 µg of antibody at 4°C overnight on a rotator and collected using a magnetic stand (Invitrogen 12321D). Immunoprecipitation was performed by resuspending antibody beads in fragmented chromatin at 4°C overnight on a rotator, then repeated washing in RIPA buffer [50 mM HEPES-KOH (pH 8), 500 mM LiCl, 1 mM EDTA (pH 8), 1% NP-40, 0.7% sodium deoxycholate, PIs] followed by a TE/50 mM NaCl wash. Elution was performed at 65°C for 15 min with elution buffer [50 mM Tris-HCl (pH 8), 10 mM EDTA (pH 8), 1% SDS] and reverse crosslinked at 65°C overnight together with input, then treated with RNAse A for 1 h at 37°C followed by 0.2 µg/ml proteinase K at 55°C for 1 h. DNA was recovered by phenol-chloroform extraction and ethanol precipitation. RT-qPCR was performed using SYBR green and AriaMx Real-Time PCR System (Agilent Technologies). Antibodies were from Abcam used at 5 µg per 25 µg of chromatin: Lsd1 (ab17721), H3K9ac (ab4441) and H3K9me2 (ab1220).

Co-immunoprecipitation

For immunoprecipitation assays, nuclear cell extracts from neuroblastoma cells were precleared in 0.5% BSA for 1 h on ice then with protein A magnetic beads for 30 min at 4°C to reduce non-specific binding and background. Precleared lysates were separated from the beads and incubated with 5 µg of antibody (anti-Lsd1, Abcam, ab17721) in co-immunoprecipitation (co-IP) buffer [20 mM Tris-HCl (pH 7.5), 100 mM NaCl, 0.2% TritonX-100, 0.2% NP-40, 2 mM β-mercaptoethanol, 0.2% sodium deoxycholate, 1 mM DTT, PIs] at 4°C overnight, then with beads for 4 h at 4°C followed by repeated washes in wash buffer [20 mM HEPES (pH 7.5), 1.25 mM $MgCl_2$, 0.1 mM EDTA (pH 8), 10% glycerol, 0.2% NP-40, 100 mM KCl, 1 mM DTT, PIs]. Beads were collected, resuspended in 2× SDS loading buffer, boiled for 5 min at 95°C and run on SDS-PAGE gel for western blotting.

Western blot

Protein lysates from neuroblastoma cells were separated by SDS-PAGE and transferred onto PVDF membranes using a Bio-Rad Trans-blot Turbo transfer system. After blocking, the membranes were incubated with primary antibody (anti-cMyb, Abcam, ab45150 at 1:2500 or anti-Lsd1, Abcam, ab17721 at 1:1000) overnight at 4°C followed by PBST washes and incubation with HRP-conjugated secondary antibody (Jackson Labs, 1:10,000) for 2 h. Signals were visualized using Bio-Rad Clarity Western ECL Substrate and Bio-Rad ChemiDoc Touch imaging system.

ChIP-qPCR data and statistical analysis

Input Ct values were adjusted for the dilution factor and ΔCt calculated by normalizing Ct values to the adjusted input: ΔCt=Ct(input)-Ct(IP). The % input was calculated as % input=$100\times2e^{-\Delta Ct}$. Fold enrichment was calculated using % input of IP/IgG: [ΔCt(IP)/ΔCt(IgG]. Error bars

Development (2018) 145, dev160325. doi:10.1242/dev.160325

represent the standard error. Unless otherwise indicated, differences between experimental groups were compared using an unpaired two-tailed Student's *t*-test and $P \leq 0.05$ was considered statistically significant.

Fluorescence quantification

ImageJ was used to measure the integrated density (fluorescence intensity) in the region of interest for both electroporated and drug-treated samples. For electroporated cells, the mean fluorescence intensity of targeted cells/Hoechst was compared with non-targeted cells/Hoechst, whereas for drug-treated versus untreated samples, the entire placode/Hoechst was measured. To correct for different exposure levels between channels and individual samples, the integrated density from the mean of three background areas was also calculated. The formula used to estimate the corrected total cell fluorescence (CTCF) was as follows: integrated density–(area of selection×mean fluorescence of background reading). Statistical significance was estimated using an unpaired *t*-test.

Motif enrichment analysis

Transcription factor-binding motifs were predicted using the JASPAR database (jaspar.genereg.net) and P-Match program from the Transfac database (www.gene-regulation.com/pub/programs.html). A profile matrix was generated to run a pattern matching scan using RSAT (rsat.sb-roscoff.fr/) on the promoters for enrichment against the background (chicken genome).

Pharmacological inhibition

Dissected OEP tissues were cultured in collagen with trans-2-phenylcyclopropylamine (tranylcypromine, TCP, at 25 µm working concentration prepared in sterile water) in culture medium. Explants were incubated with drug (or no drug control) for 30 min at room temperature before culturing for either 4.5 or 9 h. For sectioning and immunofluorescence, the whole embryo or head was cultured in the presence or absence of drug for 12 h on polycarbonate membranes (Corning, 3422).

In ovo electroporation and tissue dissection

Fertilized hen's eggs (Winter Farm, Hertfordshire, UK) were incubated in a humidified incubator at 38°C to reach ss5-6. Eggs were windowed and embryos visualized using India ink (Pelikan; diluted 1:5 in Tyrode's saline). The positive (platinum) electrode was placed under the embryo at hindbrain (r4) level, DNA/morpholino was injected below the vitelline membrane, the negative (tungsten) electrode was placed on top and the current was applied using an Intracel electroporator (settings: 5 V, 5 pulses, 50 ms, 10 ms duration). Tyrode's saline supplemented with penicillin streptomycin was applied to the embryo, the egg was resealed with tape and incubated to the appropriate stage. Placodes were dissected as described previously (Anwar et al., 2017; Chen et al., 2017).

In situ hybridization and immunofluorescence

Embryos were fixed in 4% paraformaldehyde (PFA) overnight at 4°C and *in situ* hybridization performed using DIG-labelled riboprobes. For antibody staining, embryos were embedded in paraffin wax or gelatine and sectioned at 8 µm. Primary antibodies used were: anti-H3K9ac (Abcam, ab4441) 1:100; anti-H3K9me2 (Abcam, ab1220) 1:100; anti-FITC 488 (Thermo Scientific, 4-4-20) 1:500; anti-mCherry (Abcam, ab167453) 1:500; anti-cleaved caspase 3 (Cell Signaling, 9964B) 1:300; and anti-Lsd1 (Abcam, ab17721) 1:300. Secondary antibodies were: goat anti-rabbit or anti-mouse Alexa Fluor 568 (1:1000, Invitrogen) and Alexa Fluor 635 (1:500, Invitrogen).

Morpholinos and DNA constructs

Fluoresceinated morpholino antisense oligonucleotides were obtained from Gene Tools with standard Ctrl-MO (5′-CCTCTTACCTCAGTTAC-AATTTATA-3′) from the manufacturer and cMyb-MO (5′-ATGGCCGC-GAGCTCCGCGTGCAGAT-3′) published by Betancur et al. (2011). Both Lsd1 morpholinos were splice morpholinos. Lsd1-MO 1 (5′-TTTGTGAAACTCACCAAGTCCTGTT-3′) deletes exon 8 (enzymatic domain). Lsd1-MO 2 (5′-ATCACTGGACAAAATCTGACCTTGT-3′) deletes exon 11 (substrate-binding domain). All morpholinos were used at a 1 mM final concentration. Lsd1-RFP expression constructs were generated by subcloning the human Lsd1 (a gift from Prof. Yang Shi, Harvard Medical School, Boston, MA, USA) open reading frame into pCAB.IRES.RFP vector.

Quantitative RT-PCR and NanoString nCounter analysis

Preparation of tissue for qPCR and NanoString analysis were conducted as previously described (Anwar et al., 2017; Chen et al., 2017).

Acknowledgements

We thank Rosalinda Guerra and Ewa Kolano for excellent technical support. We thank Prof. Claudio Stern, Dr Albert Basson, Dr Ravindra Prajapati and Dr Mark Hintze for comments on the manuscript; Dr Karen Liu and Daniel Doro Pereira for cell lines; and Prof. Yang Shi (Harvard Medical School). The authors declare no competing or financial interests.

Author contributions

Conceptualization: M.A., A.S.; Investigation: M.A.; Data curation: M.A., A.S.; Writing - original draft: M.A., A.S.; Writing - review & editing: M.A.; Supervision: A.S.; Project administration: A.S.; Funding acquisition: A.S.

Funding

This work was supported by grant to A.S. by the Biotechnology and Biological Sciences Research Council (BB/I021647/1 and BB/M006964) and the National Institute on Deafness and Other Communication Disorders (DC011577). Deposited in PMC for release after 6 months.

Supplementary information

Supplementary information available online at
http://dev.biologists.org/lookup/doi/10.1242/dev.160325.supplemental

References

Adamo, A., Sesé, B., Boue, S., Castaño, J., Paramonov, I., Barrero, M. J. and Belmonte, J. C. I. (2011). LSD1 regulates the balance between self-renewal and differentiation in human embryonic stem cells. *Nat. Cell Biol.* **13**, 652-659.

Anwar, M., Tambalo, M., Ranganathan, R., Grocott, T. and Streit, A. (2017). A gene network regulated by FGF signalling during ear development. *Sci. Rep.* **7**, 6162.

Bailey, A. P., Bhattacharyya, S., Bronner-Fraser, M. and Streit, A. (2006). Lens specification is the ground state of all sensory placodes, from which FGF promotes olfactory identity. *Dev. Cell* **11**, 505-517.

Ballas, N., Grunseich, C., Lu, D. D., Speh, J. C. and Mandel, G. (2005). REST and its corepressors mediate plasticity of neuronal gene chromatin throughout neurogenesis. *Cell* **121**, 645-657.

Barski, A., Cuddapah, S., Cui, K., Roh, T.-Y., Schones, D. E., Wang, Z., Wei, G., Chepelev, I. and Zhao, K. (2007). High-resolution profiling of histone methylations in the human genome. *Cell* **129**, 823-837.

Betancur, P., Sauka-Spengler, T. and Bronner, M. (2011). A Sox10 enhancer element common to the otic placode and neural crest is activated by tissue-specific paralogs. *Development (Cambridge, England)* **138**, 3689-3698.

Bhattacharyya, S., Bailey, A. P., Bronner-Fraser, M. and Streit, A. (2004). Segregation of lens and olfactory precursors from a common territory: cell sorting and reciprocity of Dlx5 and Pax6 expression. *Dev. Biol.* **271**, 403-414.

Boyer, L. A., Latek, R. R. and Peterson, C. L. (2004). The SANT domain: a unique histone-tail-binding module? *Nat. Rev. Mol. Cell Biol.* **5**, 158-163.

Chen, Y., Kim, J., Zhang, R., Yang, X., Zhang, Y., Fang, J., Chen, Z., Teng, L., Chen, X., Ge, H. et al. (2016). Histone demethylase LSD1 promotes adipocyte differentiation through repressing Wnt signaling. *Cell Chem. Biol.* **23**, 1228-1240.

Chen, J., Tambalo, M., Barembaum, M., Ranganathan, R., Simões-Costa, M., Bronner, M. E. and Streit, A. (2017). A systems-level approach reveals new gene regulatory modules in the developing ear. *Development (Cambridge, England)* **144**, 1531-1543.

Chong, J. X., Yu, J.-H., Lorentzen, P., Park, K. M., Jamal, S. M., Tabor, H. K., Rauch, A., Saenz, M. S., Boltshauser, E., Patterson, K. E. et al. (2016). Gene discovery for Mendelian conditions via social networking: de novo variants in KDM1A cause developmental delay and distinctive facial features. *Genet. Med.* **18**, 788-795.

Forneris, F., Binda, C., Dall'Aglio, A., Fraaije, M. W., Battaglioli, E. and Mattevi, A. (2006). A highly specific mechanism of histone H3-K4 recognition by histone demethylase LSD1. *J. Biol. Chem.* **281**, 35289-35295.

Foster, C. T., Dovey, O. M., Lezina, L., Luo, J. L., Gant, T. W., Barlev, N., Bradley, A. and Cowley, S. M. (2010). Lysine-specific demethylase 1 regulates the embryonic transcriptome and CoREST stability. *Mol. Cell. Biol.* **30**, 4851-4863.

Freter, S., Muta, Y., Mak, S.-S., Rinkwitz, S. and Ladher, R. K. (2008). Progressive restriction of otic fate: the role of FGF and Wnt in resolving inner ear potential. *Development* **135**, 3415.

Groves, A. K. and Bronner-Fraser, M. (2000). Competence, specification and commitment in otic placode induction. *Development* **127**, 3489.
He, Y., Tang, D., Cai, C., Chai, R. and Li, H. (2016). LSD1 is required for hair cell regeneration in zebrafish. *Mol. Neurobiol.* **53**, 2421-2434.
Huang, Z., Li, S., Song, W., Li, X., Li, Q., Zhang, Z., Han, Y., Zhang, X., Miao, S., Du, R. et al. (2013). Lysine-specific demethylase 1 (LSD1/KDM1A) contributes to colorectal tumorigenesis via activation of the Wnt/B-catenin pathway by down-regulating dickkopf-1 (DKK1). *PLoS ONE* **8**, e70077.
Huang, M., Chen, C., Geng, J., Han, D., Wang, T., Xie, T., Wang, L., Wang, Y., Wang, C., Lei, Z. et al. (2017). Targeting KDM1A attenuates Wnt/b-catenin signaling pathway to eliminate sorafenib-resistant stem-like cells in hepatocellular carcinoma. *Cancer Lett.* **398**, 12-21.
Jayasena, C. S., Ohyama, T., Segil, N. and Groves, A. K. (2008). Notch signaling augments the canonical Wnt pathway to specify the size of the otic placode. *Development (Cambridge, England)* **135**, 2251-2261.
Karmodiya, K., Krebs, A. R., Oulad-Abdelghani, M., Kimura, H. and Tora, L. (2012). H3K9 and H3K14 acetylation co-occur at many gene regulatory elements, while H3K14ac marks a subset of inactive inducible promoters in mouse embryonic stem cells. *BMC Genomics* **13**, 424-424.
Kee, Y. and Bronner-Fraser, M. (2001). Id4 expression and its relationship to other Id genes during avian embryonic development. *Mech. Dev.* **109**, 341-345.
Labbé, R. M., Holowatyj, A. and Yang, Z.-Q. (2014). Histone lysine demethylase (KDM) subfamily 4: structures, functions and therapeutic potential. *Am. J. Transl. Res.* **6**, 1-15.
Ladher, R. K., Anakwe, K. U., Gurney, A. L., Schoenwolf, G. C. and Francis-West, P. H. (2000). Identification of synergistic signals initiating inner ear development. *Science* **290**, 1965.
Laurent, B., Ruitu, L., Murn, J., Hempel, K., Ferrao, R., Xiang, Y., Liu, S., Garcia, B. A., Wu, H., Wu, F. et al. (2015). A Specific LSD1/KDM1A isoform regulates neuronal differentiation through H3K9 demethylation. *Mol. Cell* **57**, 957-970.
Layman, W. S. and Zuo, J. (2014). Epigenetic regulation in the inner ear and its potential roles in development, protection, and regeneration. *Front. Cell. Neurosci.* **8**, 446.
Lecoin, L., Sii-Felice, K., Pouponnot, C., Eychène, A. and Felder-Schmittbuhl, M.-P. (2004). Comparison of maf gene expression patterns during chick embryo development. *Gene Expr. Patterns* **4**, 35-46.
Lee, M. G., Wynder, C., Cooch, N. and Shiekhattar, R. (2005). An essential role for CoREST in nucleosomal histone 3 lysine 4 demethylation. *Nature* **437**, 432-435.
Lei, Z.-J., Wang, J., Xiao, H.-L., Guo, Y., Wang, T., Li, Q., Liu, L., Luo, X., Fan, L.-L., Lin, L. et al. (2015). Lysine-specific demethylase 1 promotes the stemness and chemoresistance of Lgr5+ liver cancer initiating cells by suppressing negative regulators of [beta]-catenin signaling. *Oncogene* **34**, 3188-3198.
Lin, Y., Wu, Y., Li, J., Dong, C., Ye, X., Chi, Y.-I., Evers, B. M. and Zhou, B. P. (2010). The SNAG domain of Snail1 functions as a molecular hook for recruiting lysine-specific demethylase 1. *EMBO J.* **29**, 1803-1816.
Lunn, J. S., Fishwick, K. J., Halley, P. A. and Storey, K. G. (2007). A spatial and temporal map of FGF/Erk1/2 activity and response repertoires in the early chick embryo. *Dev. Biol.* **302**, 536-552.
Maroon, H., Walshe, J., Mahmood, R., Kiefer, P., Dickson, C. and Mason, I. (2002). Fgf3 and Fgf8 are required together for formation of the otic placode and vesicle. *Development* **129**, 2099.
Martin, K. and Groves, A. K. (2006). Competence of cranial ectoderm to respond to Fgf signaling suggests a two-step model of otic placode induction. *Development* **133**, 877.
Martin, C. and Zhang, Y. (2005). The diverse functions of histone lysine methylation. *Nat. Rev. Mol. Cell Biol.* **6**, 838-849.
McKeown, S. J., Lee, V. M., Bronner-Fraser, M., Newgreen, D. F. and Farlie, P. G. (2005). Sox10 overexpression induces neural crest-like cells from all dorsoventral levels of the neural tube but inhibits differentiation. *Dev. Dyn.* **233**, 430-444.
Metzger, E., Wissmann, M., Yin, N., Müller, J. M., Schneider, R., Peters, A. H. F. M., Günther, T., Buettner, R. and Schüle, R. (2005). LSD1 demethylates repressive histone marks to promote androgen-receptor-dependent transcription. *Nature* **437**, 436-439.
Metzger, E., Willmann, D., McMillan, J., Forne, I., Metzger, P., Gerhardt, S., Petroll, K., von Maessenhausen, A., Urban, S., Schott, A.-K. et al. (2016). Assembly of methylated KDM1A and CHD1 drives androgen receptor-dependent transcription and translocation. *Nat. Struct. Mol. Biol.* **23**, 132-139.
Mo, X., Kowenz-Leutz, E., Laumonnier, Y., Xu, H. and Leutz, A. (2005). Histone H3 tail positioning and acetylation by the c-Myb but not the v-Myb DNA-binding SANT domain. *Genes Dev.* **19**, 2447-2457.
Musri, M. M., Carmona, M. C., Hanzu, F. A., Kaliman, P., Gomis, R. and Párrizas, M. (2010). Histone demethylase LSD1 regulates adipogenesis. *J. Biol. Chem.*. **285**, 30034-30041.
Nechiporuk, A., Linbo, T., Poss, K. D. and Raible, D. W. (2007). Specification of epibranchial placodes in zebrafish. *Development* **134**, 611.
Nieto, M. A. (2002). The snail superfamily of zinc-finger transcription factors. *Nat. Rev. Mol. Cell Biol.* **3**, 155-166.
Ooi, L. and Wood, I. C. (2007). Chromatin crosstalk in development and disease: lessons from REST. *Nat. Rev. Genet.* **8**, 544-554.
Park, B.-Y. and Saint-Jeannet, J.-P. (2008). Hindbrain-derived Wnt and Fgf signals cooperate to specify the otic placode in Xenopus. *Dev. Biol.* **324**, 108-121.
Phillips, B. T., Bolding, K. and Riley, B. B. (2001). Zebrafish fgf3 and fgf8 encode redundant functions required for otic placode induction. *Dev. Biol.* **235**, 351-365.
Popova, E. Y., Pinzon-Guzman, C., Salzberg, A. C., Zhang, S. S.-M. and Barnstable, C. J. (2016). LSD1-mediated demethylation of H3K4me2 is required for the transition from late progenitor to differentiated mouse rod photoreceptor. *Mol. Neurobiol.* **53**, 4563-4581.
Saleque, S., Kim, J., Rooke, H. M. and Orkin, S. H. (2007). Epigenetic regulation of hematopoietic differentiation by Gfi-1 and Gfi-1b is mediated by the cofactors CoREST and LSD1. *Mol. Cell* **27**, 562-572.
Schmidt, D. M. Z. and McCafferty, D. G. (2007). trans-2-phenylcyclopropylamine is a mechanism-based inactivator of the histone demethylase LSD1. *Biochemistry* **46**, 4408-4416.
Sheng, G. and Stern, C. D. (1999). Gata2 and Gata3: novel markers for early embryonic polarity and for non-neural ectoderm in the chick embryo. *Mech. Dev.* **87**, 213-216.
Sheng, G., dos Reis, M. and Stern, C. D. (2003). Churchill, a zinc finger transcriptional activator, regulates the transition between gastrulation and neurulation. *Cell* **115**, 603-613.
Shi, Y., Sawada, J.-i., Sui, G., Affar, E. B., Whetstine, J. R., Lan, F., Ogawa, H., Po-Shan Luke, M., Nakatani, Y. and Shi, Y. (2003). Coordinated histone modifications mediated by a CtBP co-repressor complex. *Nature* **422**, 735-738.
Shi, Y.-J., Matson, C., Lan, F., Iwase, S., Baba, T. and Shi, Y. (2005). Regulation of LSD1 histone demethylase activity by its associated factors. *Mol. Cell* **19**, 857-864.
Shida, H., Mende, M., Takano-Yamamoto, T., Osumi, N., Streit, A. and Wakamatsu, Y. (2015). Otic placode cell specification and proliferation are regulated by Notch signaling in avian development. *Dev. Dyn.* **244**, 839-851.
Streit, A. (2002). Extensive cell movements accompany formation of the otic placode. *Dev. Biol.* **249**, 237-254.
Sun, S.-K., Dee, C. T., Tripathi, V. B., Rengifo, A., Hirst, C. S. and Scotting, P. J. (2007). Epibranchial and otic placodes are induced by a common Fgf signal, but their subsequent development is independent. *Dev. Biol.* **303**, 675-686.
Sun, G., Alzayady, K., Stewart, R., Ye, P., Yang, S., Li, W. and Shi, Y. (2010). Histone demethylase LSD1 regulates neural stem cell proliferation. *Mol. Cell. Biol.* **30**, 1997-2005.
Takeuchi, M., Fuse, Y., Watanabe, M., Andrea, C.-S., Takeuchi, M., Nakajima, H., Ohashi, K., Kaneko, H., Kobayashi-Osaki, M., Yamamoto, M. et al. (2015). LSD1/KDM1A promotes hematopoietic commitment of hemangioblasts through downregulation of Etv2. *Proc. Natl. Acad. Sci. USA* **112**, 13922-13927.
Thambyrajah, R., Mazan, M., Patel, R., Moignard, V., Stefanska, M., Marinopoulou, E., Li, Y., Lancrin, C., Clapes, T., Moroy, T. et al. (2016). GFI1 proteins orchestrate the emergence of haematopoietic stem cells through recruitment of LSD1. *Nat. Cell Biol.* **18**, 21-32.
Tsai, M.-C., Manor, O., Wan, Y., Mosammaparast, N., Wang, J. K., Lan, F., Shi, Y., Segal, E. and Chang, H. Y. (2010). Long noncoding RNA as modular scaffold of histone modification complexes. *Science (New York, N.Y.)* **329**, 689-693.
Tunovic, S., Barkovich, J., Sherr, E. H. and Slavotinek, A. M. (2014). De novo ANKRD11 and KDM1A gene mutations in a male with features of KBG syndrome and Kabuki syndrome. *Am. J. Med Genet. A* **164**, 1744-1749.
Uribe, R. A., Buzzi, A. L., Bronner, M. E. and Strobl-Mazzulla, P. H. (2015). Histone demethylase KDM4B regulates otic vesicle invagination via epigenetic control of Dlx3 expression. *J. Cell Biol.* **211**, 815-827.
Urness, L. D., Paxton, C. N., Wang, X., Schoenwolf, G. C. and Mansour, S. L. (2010). FGF signaling regulates otic placode induction and refinement by controlling both ectodermal target genes and hindbrain Wnt8a. *Dev. Biol.* **340**, 595-604.
Wang, J., Scully, K., Zhu, X., Cai, L., Zhang, J., Prefontaine, G. G., Krones, A., Ohgi, K. A., Zhu, P., Garcia-Bassets, I. et al. (2007). Opposing LSD1 complexes function in developmental gene activation and repression programmes. *Nature* **446**, 882-887.
Wright, T. J. and Mansour, S. L. (2003). Fgf3 and Fgf10 are required for mouse otic placode induction. *Development* **130**, 3379.
Yang, L., O'Neill, P., Martin, K., Maass, J. C., Vassilev, V., Ladher, R. and Groves, A. K. (2013). Analysis of FGF-dependent and FGF-independent pathways in otic placode Induction. *PLoS ONE* **8**, e55011.
Zibetti, C., Adamo, A., Binda, C., Forneris, F., Toffolo, E., Verpelli, C., Ginelli, E., Mattevi, A., Sala, C. and Battaglioli, E. (2010). Alternative splicing of the histone demethylase LSD1/KDM1 contributes to the modulation of neurite morphogenesis in the mammalian nervous system. *J. Neurosci.* **30**, 2521.

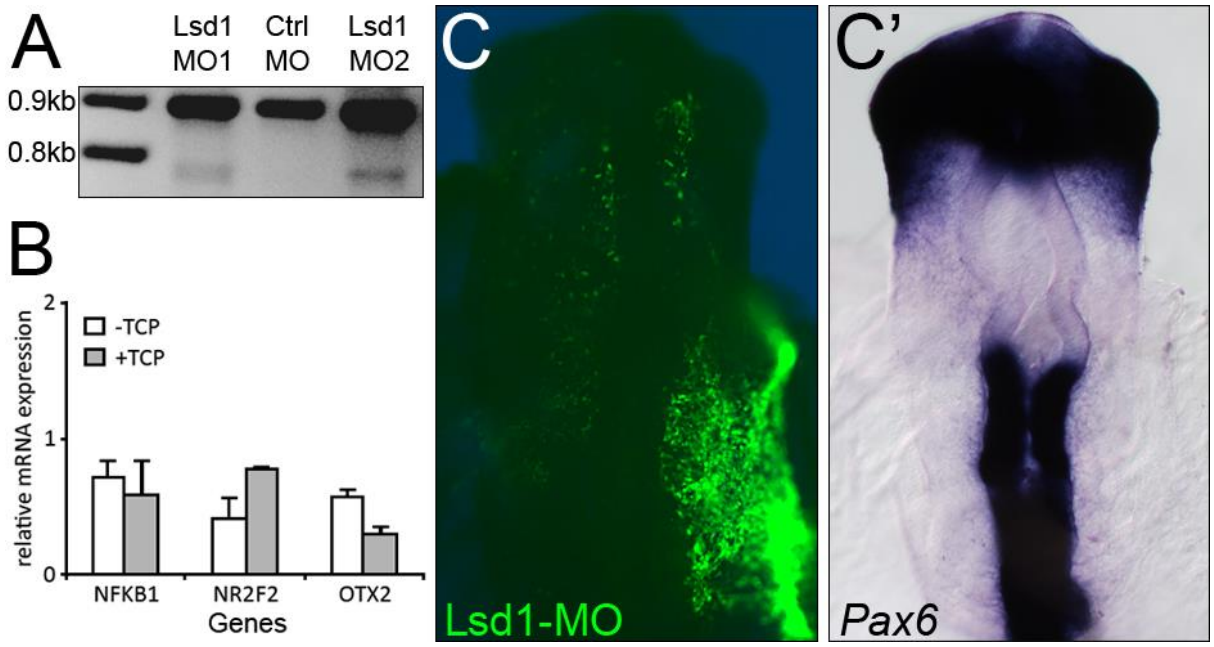

Fig. S1. Lsd1 splice morpholinos and validation of non-otic genes. (A) RT-PCR. Lsd1-MO1 deletes exon 8 and generates an amplicon 95bp smaller than the wild type (top band). Lsd1-MO2 deletes exon 11 and generates an amplicon 91bp smaller than the wild type. (B) Validation of selected upregulated genes by qPCR following pharmacological inhibition of Lsd1 with TCP, normalised to *Sdha*. There is no significant difference between drug treated vs untreated samples. (C) Electroporation of Lsd1-MO (green) and (C') ISH for *Pax6*, an upregulated gene. Note that upregulation of *Pax6* is not observed (n=5).

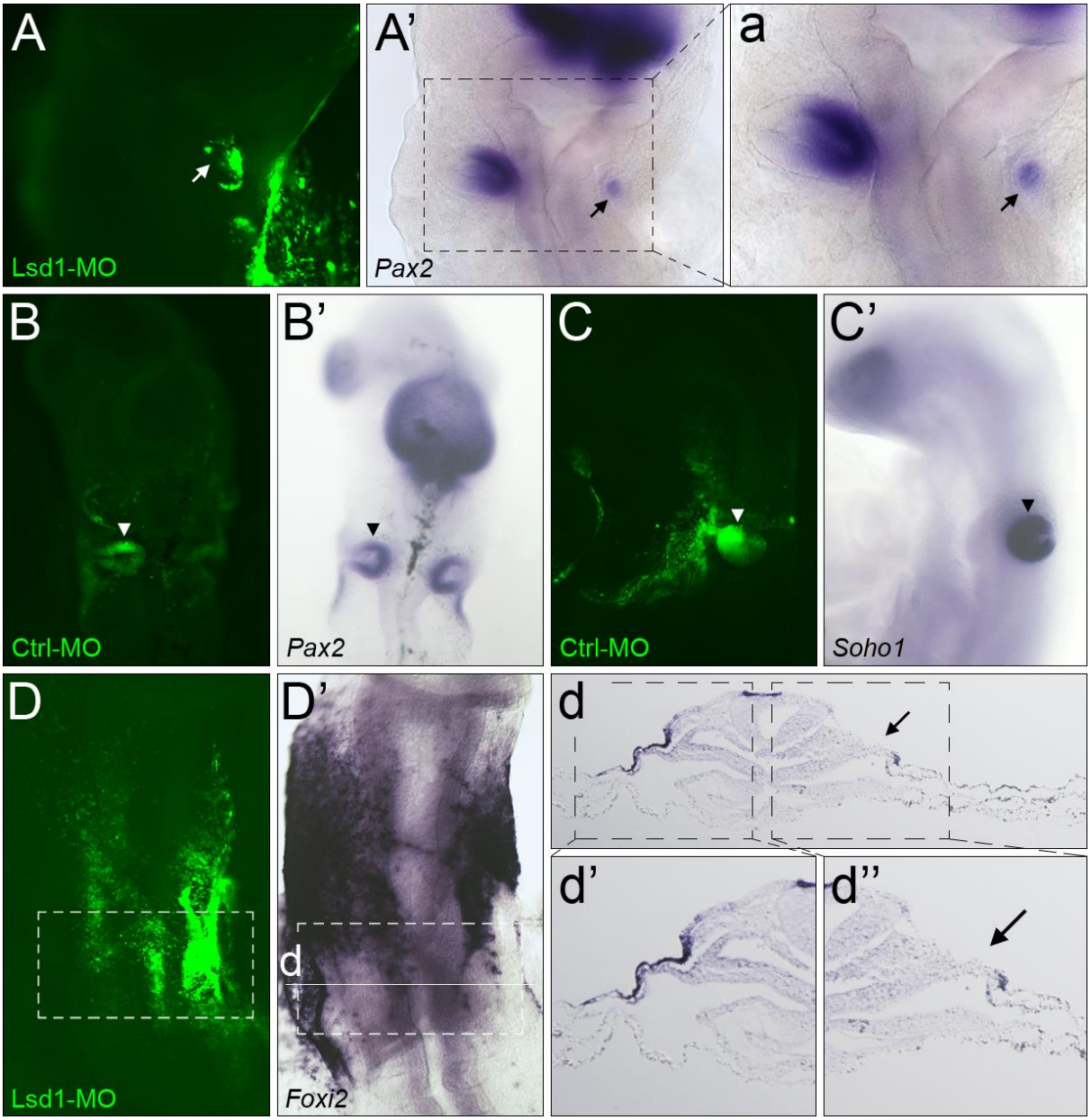

Fig. S2. Lsd1-MO knockdown prevents otic vesicle formation. (A-a) Otic cells electroporated with Lsd1-MO (green) do not express *Pax2* and are unable to form an otic vesicle compared to cells that did not receive the Lsd1-MO (arrow) which continue to express *Pax2*. (B-C') Electroporation of control (Ctrl) –MO does not affect marker gene expression or otic vesicle formation (arrowhead). (D-d") Electroporation of Lsd1-MO in epibranchial regions leads to a reduction in *Foxi2* expression. Arrow indicates electroporated side. (d', d") zoomed images of area inside dashed boxes in panel d.

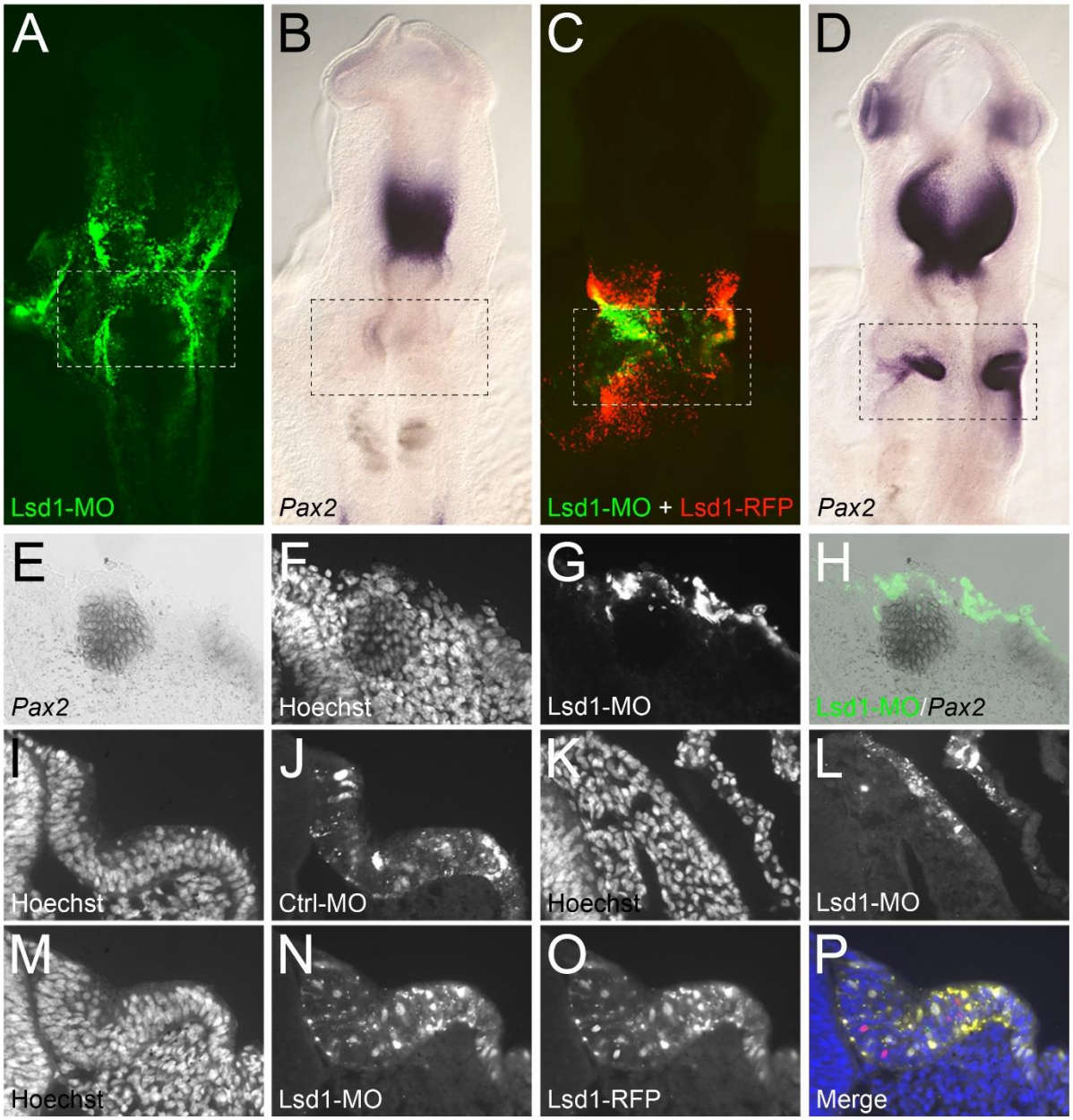

Fig. S3. Lsd1 expression rescues otic placode formation after Lsd1-MO knockdown. (A, B) Lsd1-MO causes loss of placode formation and *Pax2* expression. (C-D) Co-electroporation of Lsd1-MO with full length human Lsd1-RFP rescues *Pax2* expression and subsequent otic cup formation. (E-H) Lsd1-MO+ cells remain in the epithelium and do not contribute to vesicle formation unlike non-targeted, *Pax2+* cells. (I, J) Ctrl-MO do not affect thickening of the otic epithelium or its invagination into an otic cup. (K, L) Lsd1-MO prevents both the thickening and invagination of the epithelium, while co-electroporation of Lsd1-RFP together with Lsd1-MO restores normal morphology (M-P). Hoechst = nuclei.

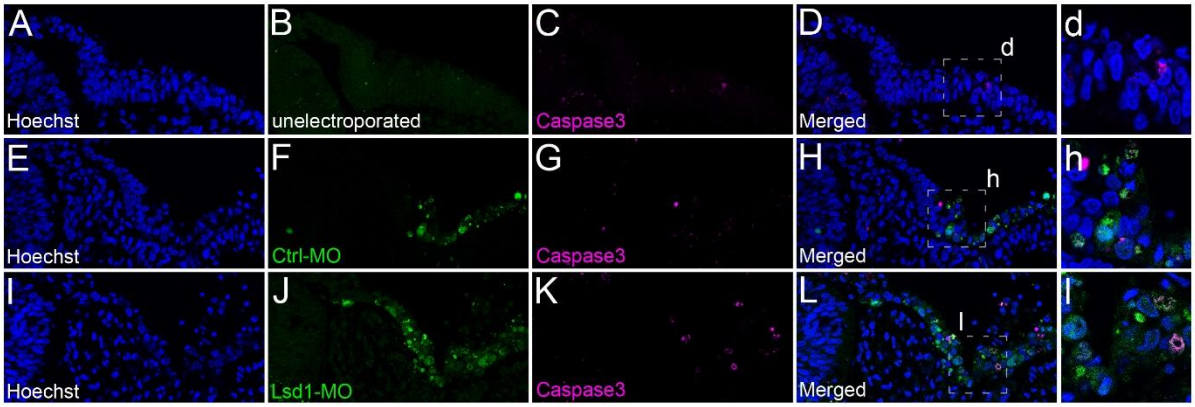

Fig. S4. Lsd1-MO knockdown does not lead to increased apoptosis. (A-d) Unelectroporated placode showing some cleaved caspase 3^{+} cells. (E-h) Ctrl-MO and (I-l) Lsd1-MO show similar levels of apoptotic cells.

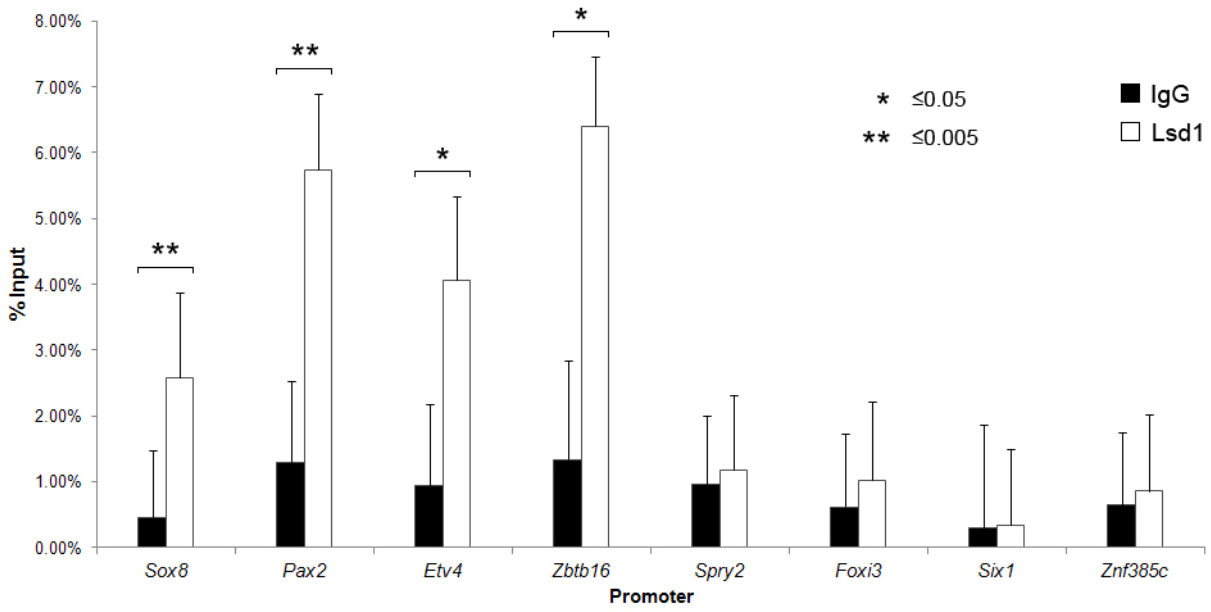

Fig. S5. Lsd1 binding to target otic gene promoters. Lsd1 ChIP-qPCR for OEP and PPR genes shown in Fig4A is represented here as % input. Lsd1 only occupies the promoters of OEP genes.

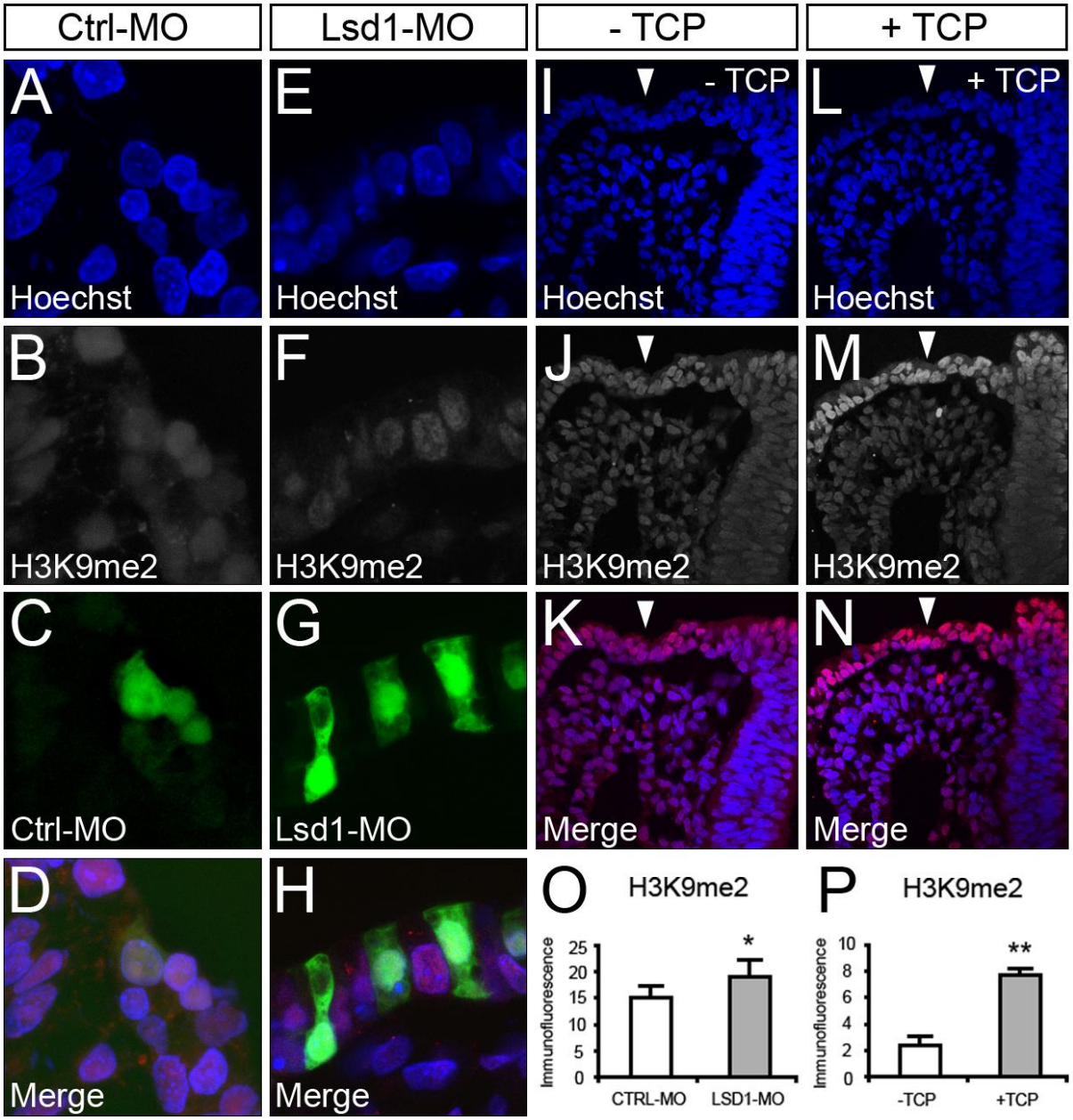

Fig. S6. Lsd1 inhibition increases H3K9me2 in the otic placode. (A-D) Ctrl-MO and (E-H) Lsd1-MO electroporation into the otic region. Nuclei are visualised with Hoechst (blue), H3K9me2 immunofluorescence in grey and MO targeted cells in green. (D, H) Merged images. (I-K) Control (-TCP) and (L-N) TCP treated otic explants showing Hoechst stained nuclei (blue) and H3K9me2 (grey). (K, N) Merged images. Arrowheads point to the epithelium. (O, P) ImageJ was used to measure the intensity of H3K9me2 fluorescence (B, F, J, M) in cells targeted with MO (green) and their neighbours (O) and in TCP treated and untreated epithelium (P). Note that in both morpholino and drug mediated inhibition of Lsd1, there is a significant increase in H3K9me2 levels (p-values: * ≤0.05; ** ≤0.01).

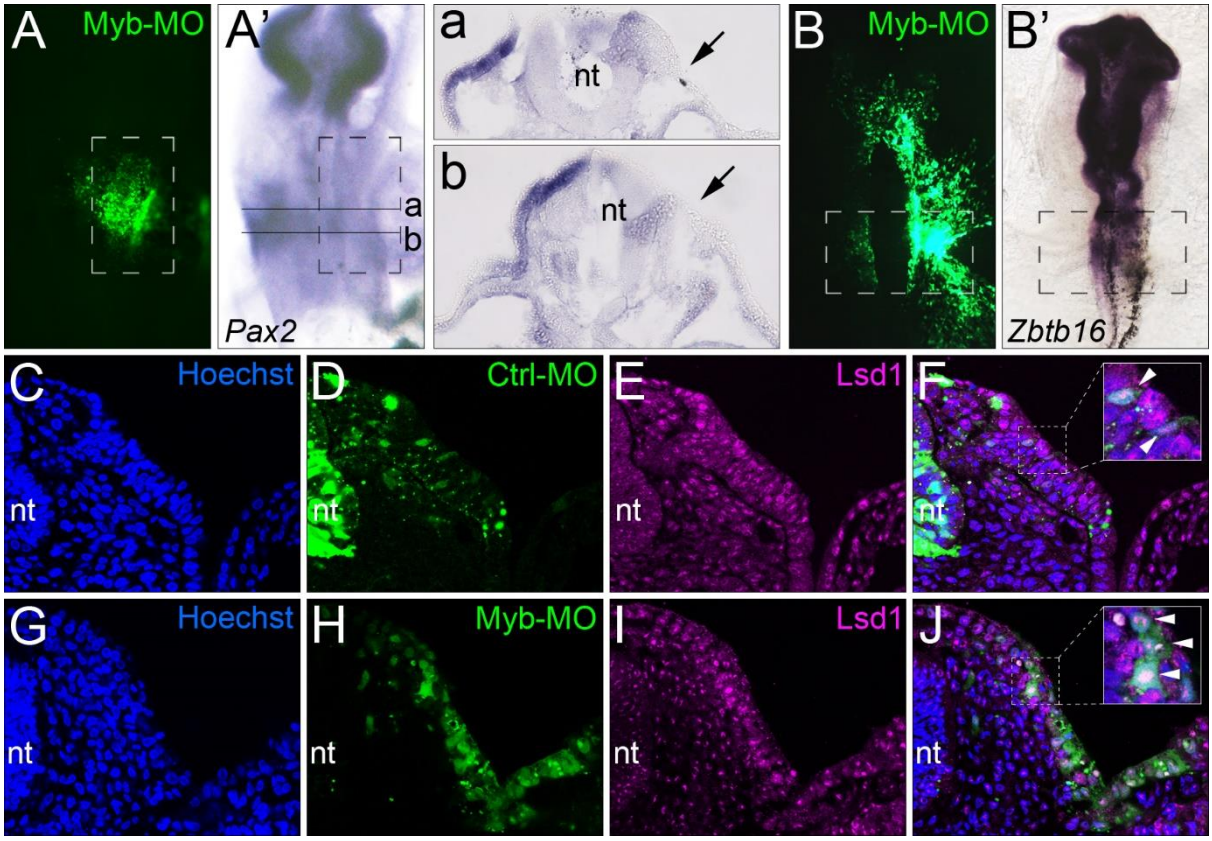

Fig. S7. Myb-MO knockdown leads to loss of otic placode markers but does not affect Lsd1 expression. (A-a) *Pax2* and (B, B') *Zbtb16* are downregulated after Myb-MO knockdown. (C-F) Ctrl-MO and (G-J) Myb-MO electroporation followed by Lsd1 antibody staining. Lsd1 is broadly expressed with slightly stronger expression in the ectoderm and placode. Arrowheads within inset depicting zoom of dashed box area indicate targeted cells. Note that Lsd1 expression persists in the nuclei of Myb-MO cells.

Supplementary Tables

Table S1. NanoString Probeset

Click here to Download Table S/

Table S2. Differential gene expression by NanoString analysis following Lsd1-MO knockdown

Click here to Download Table S0

Table S3. Motif enrichment analysis

Click here to Download Table S3